ACS OMEGA

http://pubs.acs.org/journal/acsodf

Article

Injectable Self-Setting Ternary Calcium-Based Bone Cement Promotes Bone Repair

Shengwen Cheng,[§] Chen Zhao,[§] Senrui Liu, Bowen Chen, Hong Chen, Xuefeng Luo, Li Wei, Chengcheng Du, Pengcheng Xiao, Yiting Lei,* Yonggang Yan,* and Wei Huang*

Cite This: *ACS Omega* 2023, 8, 16809−16823

Read Online

ACCESS | Metrics & More | Article Recommendations | Supporting Information

ABSTRACT: Bone defects, especially large ones, are clinically difficult to treat. The development of new bone repair materials exhibits broad application prospects in the clinical treatment of trauma. Bioceramics are considered to be one of the most promising biomaterials owing to their good biocompatibility and bone conductivity. In this study, a self-curing bone repair material having a controlled degradation rate was prepared by mixing calcium citrate, calcium hydrogen phosphate, and semi-hydrated calcium sulfate in varying proportions, and its properties were comprehensively evaluated. In vitro cell experiments and RNA sequencing showed that the composite cement activated PI3K/Akt and MAPK/Erk signaling pathways to promote osteogenesis by promoting the proliferation and osteoblastic differentiation of mesenchymal stem cells. In a rat model with femoral condyle defects, the composite bone cement showed excellent bone repair effect and promoted bone regeneration. The injectable properties of the composite cement further improved its practical applicability, and it can be applied in bone repair, especially in the repair of irregular bone defects, to achieve superior healing.

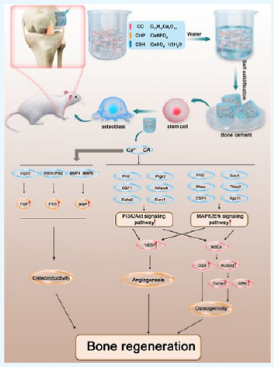

1. INTRODUCTION

Bones have a strong ability to regenerate and self-repair, especially in young people, and most bone defects heal spontaneously.[1] However, bones are unable to repair itself when a pathological fracture or large, massive bone defect occurs and requires external surgical intervention.[2] In China, the number of patients with bone defects caused by trauma, degeneration, tumors, genetic diseases, deformity, and other reasons exceeds 6 million every year, and as many as 10 million patients have limb function limitations due to bone defects.[3,4] Autogenous bone transplantation is considered the gold standard for the treatment of bone defects. The options include the iliac bone, costal cartilage, and ear cartilage. However, autologous bone transplantation may cause donor site defects, resulting in donor site pain, sensory abnormalities, infection, and other complications. Moreover, its quantity is limited; therefore, it cannot be used to repair large bone defects.[5] Hence, developing appropriate bone graft substitutes is necessary. At present, synthetic materials have become an effective treatment for diseases.[6,7]

Polymethyl methacrylate (PMMA) bone cement was first used to repair bone defects, but its biocompatibility is poor, it cannot be degraded, and it cannot achieve the growth and replacement of bone tissue.[8,9] In view of the shortcomings of PMMA bone cement, in recent years, many inorganic cements, such as calcium silicate, calcium sulfate, and hydroxyapatite, have been explored to repair bone defects. Although the mechanical strength of inorganic cements is generally lower than that of PMMA cement, they exhibit good biocompatibility and biodegradability and can achieve the growth and replacement of a new bone.[10−14] Therefore, the performance of inorganic cements needs to be further improved for achieving an ideal bone repair effect. Considering the unavoidable limitations of single-component bone cement, composite cements formed by combining a variety of organic and inorganic cements are being developed as new bone repair materials. Composite materials have good application prospects because various biological materials can be combined according to their respective properties to achieve the desired properties.

Calcium hydrogen phosphate (CHP) is similar in chemical composition to human bone mineral and also has good biocompatibility and bioactivity. However, it has a poor mechanical performance (i.e., its compressive strength is low) and degrades slowly. Therefore, its degradation performance and mechanical properties should be improved for its clinical application.[10,15] Previous studies have found that organic−inorganic components can be added to CHP to form a composite cement, thereby improving its mechanical strength and absorption rate.[16] Calcium citrate (CC), which exists in a low amount (2%) in human bones, has long been used to treat calcium deficiency. As a key intermediate metabolite of the tricarboxylic acid cycle, citrate plays a crucial role in regulating cell energy metabolism. In addition, previous studies have

Received: January 16, 2023
Accepted: April 20, 2023
Published: May 1, 2023

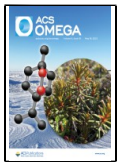

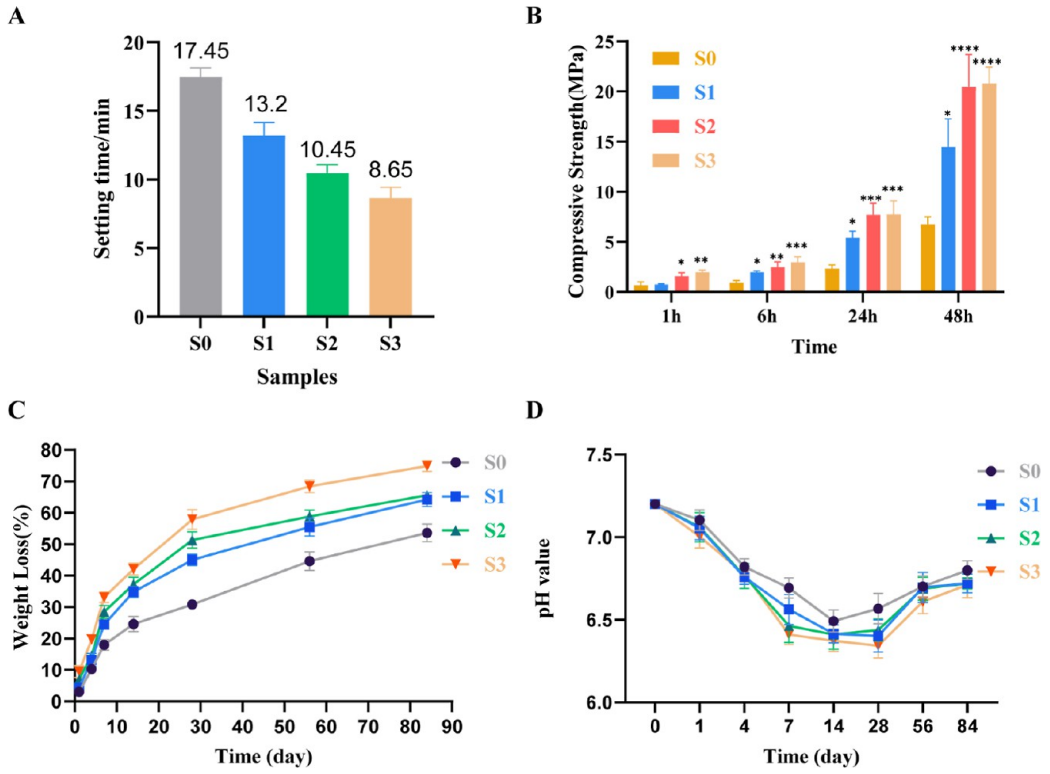

Figure 1. (A) Setting time of the bone cements with different CSH contents. (B) Compressive strength of the bone cements after setting for 1, 6, 24, and 48 h. (C) Weight loss rates of bone cements in PBS at different times. (D) PH values of bone cement in PBS at different times. (*$P < 0.05$, **$P < 0.01$, ***$P < 0.001$, and ****$P < 0.0001$, vs S0 sample, $n = 3$).

demonstrated that citric acid can promote the regeneration of defective bone.[17−19] In maxillofacial surgery, the composite cement of calcium hydrogen phosphate/calcium citrate has been used in clinics.[20] Compared with single calcium hydrophosphate, composite cement exhibits better performance (injection and degradation performance).[21,22] Further, calcium sulfate hemihydrate (CSH) is a relatively simple self-coagulation material that has long been used to fill bone defects owing to its good biocompatibility and capability to repair bones.[23,24] Calcium sulfate and calcium phosphate provide plastic surgeons with a feasible alternative to autologous bone transplantation. These materials imitate the mineral phase of bone and have good biocompatibility.[25,26] However, CSH is rapidly absorbed to allow the effective growth of new bone in the bone cavity.[20] It is, therefore, logical to combine CC, CHP, and CSH at appropriate proportions to form a composite cement to derive benefits from each component and compensate for their individual disadvantages.

In this study, we prepared composite cements with different proportions of CC, CHP, and CSH. One of the main advantages of preparing implants from such composite bone cements is the possibility of modulating the absorption rate by adjusting the CSH content. The results of this study indicate that the proposed composite cement is a fast, self-setting organic−inorganic bone repair material that promotes osteogenesis and undergoes controlled degradation.

2. RESULTS

2.1. Material Characterization. *2.1.1. Solidification and Mechanical Properties of Composite Cements.* First, the setting times of composite cements containing different amounts of CSH were determined. The setting time of the S0 cement (without CSH) was approximately 17.5 min. The condensation times of S1, S2, and S3 with different proportions of CSH were shorter than those of S0. Overall, the addition of CSH was found to accelerate the solidification of the composite cement (Figure 1A). The compressive strengths of the cements were evaluated after 1, 6, 24, and 48 h following their solidification. After 1 h of setting, the S2 and S3 composite cements with CSH had better compressive strengths than S0. As time progressed, the mechanical properties of the bone cement containing CSH differed significantly from those of S0, and the difference was considerable after 24 h. The results presented in Figure 1B indicate that the addition of CSH can effectively improve the compressive strength of the composite cement.

2.1.2. Weight Loss and pH Value. The weight losses of the composite cements with different CSH contents when soaked in phosphate buffer solution (PBS) for different durations were measured to evaluate their degradation (Figure 1C). During the first 2 weeks, all four groups exhibited a fast degradation rate. Among the different groups, the S3 group with the largest CSH content exhibited the highest degradation rate in the first 2 weeks, with its degradation reaching 42%. After 4 weeks (28 d), the S2 and S3 groups degraded by approximately 50%. In the later stages, relatively less weight loss was observed as compared to that in earlier days. The weight losses of the samples after 12 weeks were S0 (53.6%), S1 (64.2%), S2 (65.6%), and S3 (74.9%). In summary, the degradation rate of the cement was related to the CSH content. Thus, the degradation rate of the composite cement can be controlled by the addition of CSH. The greater the CSH content is, the faster the degradation rate is.

During the first 4 weeks, the pH of the immersion solution decreased gradually with increasing soaking time, and beyond 4

https://doi.org/10.1021/acsomega.3c00331
ACS Omega 2023, 8, 16809−16823

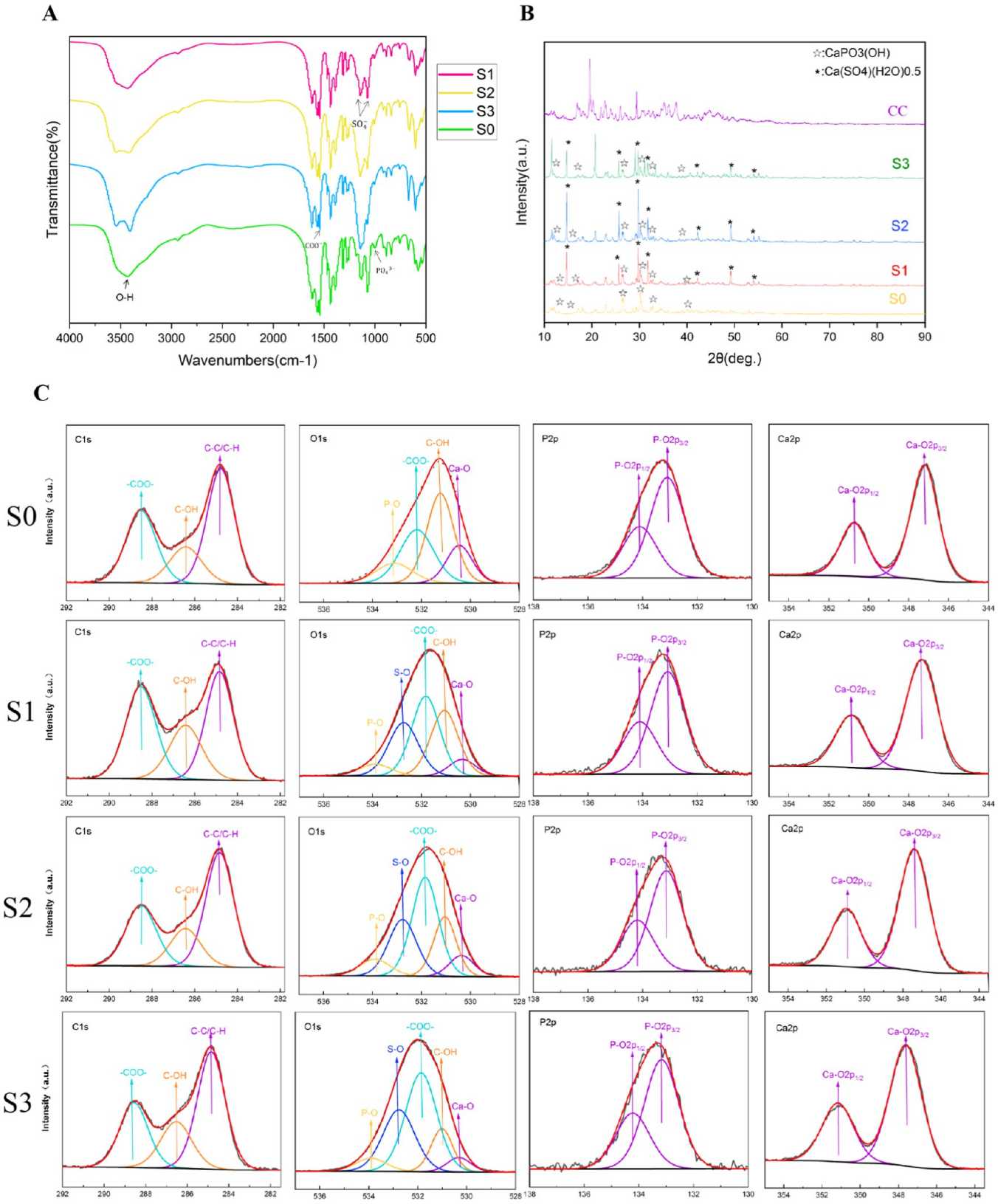

Figure 2. (A) FT-IR and (B) XRD spectra of different bone cement groups. (C) XPS profiles of the main elements of bone cements.

weeks (i.e., after 28 days), there was some recovery in pH. Compared with the pH of the immersion solution of S0 without CSH, the pH values of the solutions of the other samples were slightly lower (Figure 1D). However, the pH values of S1, S2, and S3 did not fluctuate significantly, and the pH values generally remained within the range of 6.2−7.0.

2.1.3. Structural Characterization. Figure 2A shows the FT-IR spectra of the composite cements with different CSH contents. In general, the peak types and intensities were similar

https://doi.org/10.1021/acsomega.3c00331
ACS Omega 2023, 8, 16809−16823

Table 1. Binding Energies of Major Elements in Cements

binding energy/eV	C 1s			O 1s					P 2p		Ca 2p	
S0	**284.79**	**286.34**	**288.38**	**530.45**	**531.23**	**532.19**	**533.12**		**133.1**	**134.1**	**347.21**	**350.74**
S1	284.84	286.43	288.52	530.33	531.06	531.83	533.89	532.73	134.1	134.1	347.36	350.88
S2	284.83	288.44	288.52	530.36	531.04	531.85	533.9	532.77	133.13	134.19	347.4	350.95
S3	284.9	286.64	288.63	530.38	530.9	531.74	533.88	532.83	133.22	134.22	347.57	350.97

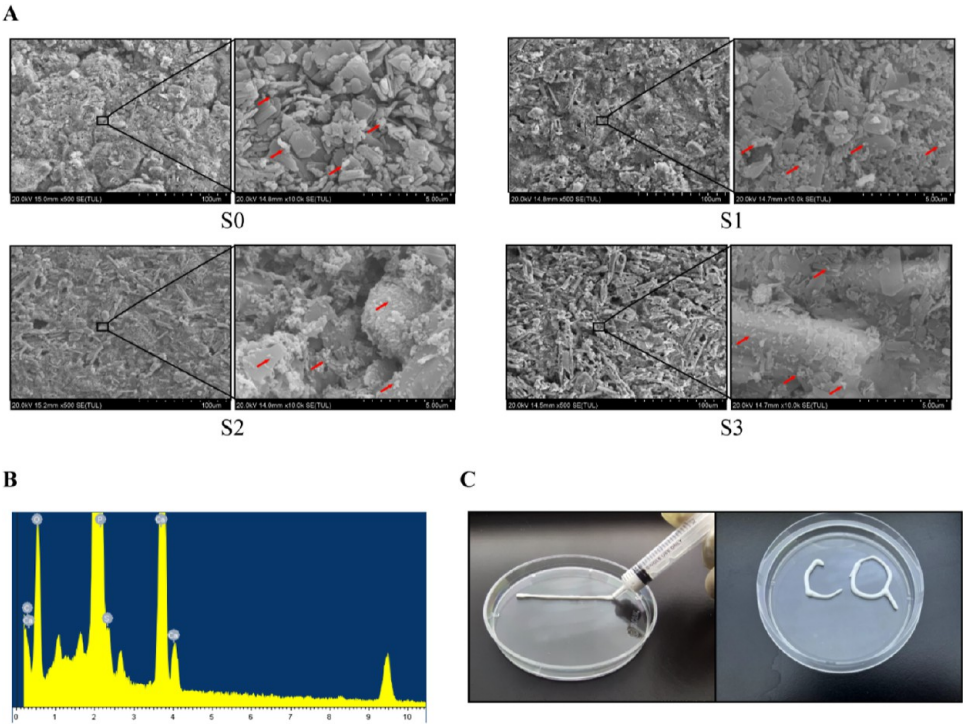

Figure 3. (A) SEM micrographs and (B) EDS spectra of bone cement samples after soaking in SBF for 7 days. (C) Injectability of bone cements.

in different groups. The characteristic absorption bands of PO_4^{3-} (946−998 cm^{-1}), COO^- (1398−1438 cm^{-1}), and SO_4^{2-} (1076−1144 cm^{-1}). The X-ray diffraction (XRD) spectra of CC and composite cements with different CSH contents are shown in the Figure 2B. The CC correlation peak almost disappeared in the XRD spectrum of the composite cement. The XRD spectrum of S0 mainly contains the peaks of CHP at 26.4, 30.1, and 32.7°. With an increase in the CSH content, the diffraction peak intensity of CHP gradually weakened compared with S0. The XRD peaks of CSH in samples S1, S2, and S3 were observed at 14.7, 25.6, 29.7, 31.7, and 49.2°. The X-ray photoelectron spectra of the composite cements are shown in Figure 2C, and the binding energy of the main elements in each cement group is summarized in Table 1. With an increase in the CSH content, the binding energy does not change uniformly, and the addition of CSH has little effect on the binding energy of other components.

2.1.4. Surface Morphology. The cements were soaked in simulated body fluid (SBF) for 7 days and observed using scanning electron microscopy (SEM). As shown in Figure 3A, a large number of white crystals (black arrows) formed on the surface of each cement group, and the main elements of the crystals, which were spherical Ca/P clusters, were further analyzed using energy dispersive X-ray spectroscopy (EDS) (Figure 3B), and the data were quantitatively analyzed (Figure S1). After 30 min of preparing the composite cements, a 5 mL syringe was used to inject the cements, and the needle was removed without blockage. This indicates that a syringe can be used to deliver bone cement to bone defects (Figure 3C), and the material can be better applied to irregular defects.

2.2. In Vitro Studies. *2.2.1. In Vitro Biocompatibility.* Figure 4A shows the results of the live/dead assay, where the spots with green and red fluorescence indicate the live and dead cells, respectively. The visual field predominantly contained live cells, with no apparent concentration of dead cells. Over time, the living cells proliferated significantly (Figure 4B), with no notable differences being observed in the early stages. However, after 3 days, the S2 and S3 cell groups exhibited increased proliferation compared to the control group. The CCK8 cell test further confirmed the exponential proliferation of the MSCs; furthermore, the experimental groups containing the extracts of the S2 and S3 cements effectively promoted the proliferation of MSCs on days 3 and 5 (Figure 4C).

2.2.2. In Vitro Osteogenic Properties of Composite Cements. Bone marrow stem cells were cultured in osteoblast media containing bone cement extracts from each group after different incubation times. The alkaline phosphatase (ALP) activity was detected through ALP staining on days 3 and 5 (Figure 5A), and calcium deposition was detected by Alizarin red staining on days 7 and 14 (Figure 5B). The ALP activity in all experimental groups was significantly higher than that in the control group. On day 7, no calcium nodules were observed in the control group. On days 7 and 14, calcium salt deposits in S1, S2, and S3 were higher than those in the control group. In particular, S2 and S3 exhibited significantly higher calcium salt deposits. These results were further confirmed by the RT-PCR

https://doi.org/10.1021/acsomega.3c00331
ACS Omega 2023, 8, 16809−16823

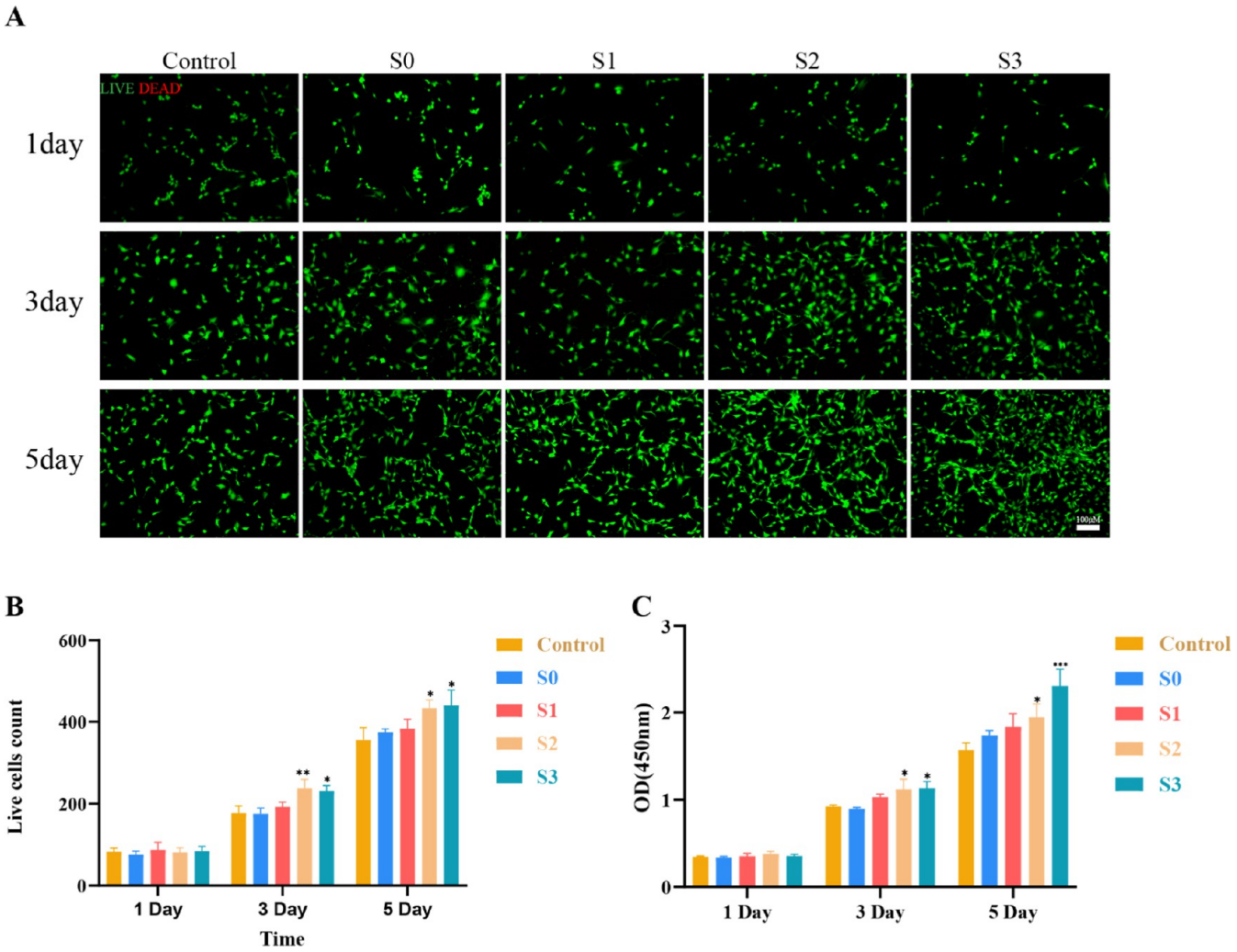

Figure 4. Proliferation of MSCs cultured with cement extracts. (A) Control group (without bone cement extract) and the bone cement extract groups with different CSH contents were tested with live/dead fluorescence stain assays. Green fluorescent cells are alive, red fluorescent cells are dead. (B) Number of living cells in the control group and each bone cement group. (C) CCK-8 assay of viability and metabolic activity of MSCs grown in the cement extracts.

analysis of the genes associated with osteogenic differentiation (collagen type I alpha 1 chain (Col1a1), osterix (OSX), osteopontin (OPN), and Runx-2) (Figure 5C). S1, S2, and S3 exhibited good osteogenic differentiation activity in vitro. Further, the Ca^{2+} and citric acid in the immersion solutions of the composite cements were analyzed by inductively coupled plasma (ICP) and ion chromatography (IC) (Figure 5D). The Ca^{2+} and citric acid contents in the immersion solutions were significantly higher in the experimental group as compared to those in the control group.

2.2.3. Mechanism of Promoted In Vitro Osteogenesis in Group S2. Gene expression in the osteoblast medium containing the extract of the S2 group composite bone cement was significantly different from that in the blank osteoblast medium, with 1820 genes upregulated and 1640 genes downregulated (Figure 6A,B). Figure 6C compares the major biological processes of the differentially expressed genes in the S2 and control groups. The expression of genes related to ossification and angiogenesis was significantly upregulated in the S2 group. The genes associated with ossification (Ror2, Fhl2, Phex, csf1, Epha2, MMP9, Itga11, P2ry2, Ptgs2, Rras2, Thbs3), angiogenesis (Notch3, Adgrb2, Ecm1, Edn1, Epha1, Nfatc4, VEgfa, Thbs2), and bone osteoinductivity (Fgf7, Pth1r, Pth2, Bmp4, Bmp6) were significantly higher in the S2 group than in the control group. These results further confirmed that the S2 group composite cement effectively promoted osteogenic differentiation by positively affecting the expression of the corresponding genes (Figure 6D). The differentially expressed genes were analyzed using the KEGG pathway enrichment analysis, and the results were sequenced. The top 10 genes are shown in Figure 6E. Finally, western blotting was performed to detect the expression levels of the related proteins, revealing that Erk expression and the p-PI3K/PI3K and p-Akt/Akt ratios increased in the S2 group (Figure 6F). In particular, the increased expression of Akt and p-Akt indicates the activation of the PI3K/Akt signaling pathway, and the high expression of Erk indicates the activation of the MAPK/Erk signaling pathway. This result was consistent with the results of the RNA sequence analysis.

2.3. In Vivo Osteogenesis Characteristics and Biological Safety of the S2 Group. *2.3.1. Micro-CT Results.* Figure S2 shows an image of the S2 composite cement when injected into the femoral condylar bone defect model of rats. Three-dimensional micro-CT was used to reconstruct femoral

https://doi.org/10.1021/acsomega.3c00331
ACS Omega 2023, 8, 16809−16823

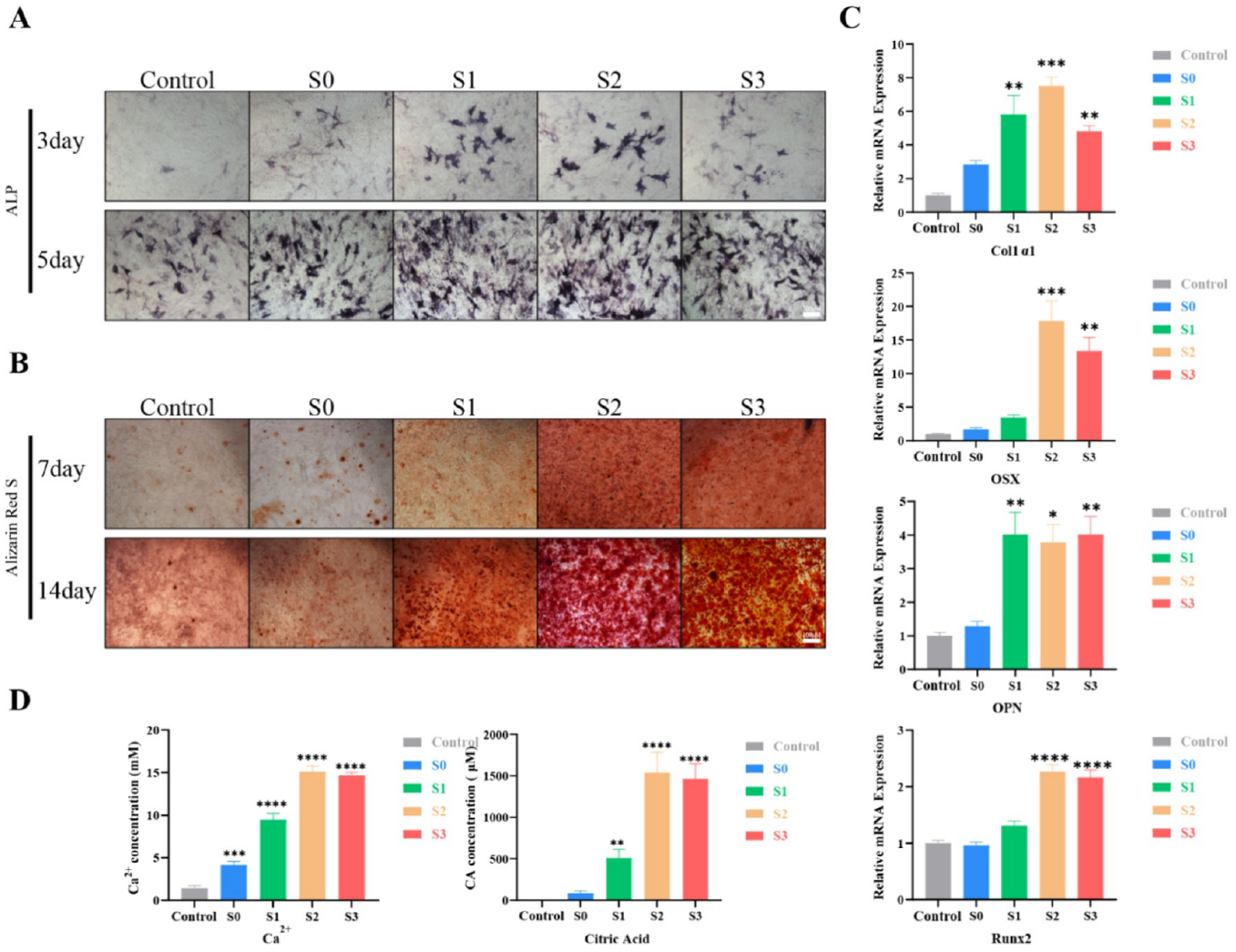

Figure 5. Osteogenic differentiation of MSCs cultured in osteogenic medium containing bone cement extract. (A) ALP staining of MSCs treated with extract solutions of S0, S1, S2, and S3 for 3 and 5 days. (B) Alizarin red staining of MSCs treated with extract solutions of S0, S1, S2, and S3 for 7 and 14 days. (C) Relative expression of osteogenic differentiation marker genes in MSCs cultured in osteogenic medium containing bone cement extract for 7 days. (D) Relative calcium ion content and citric acid concentration in osteogenic medium of each group. (*$P < 0.05$, **$P < 0.01$, ***$P < 0.001$, and ****$P < 0.0001$, vs control group, $n = 3$).

condyle defects in rats with the composite cement (Figure 7A). Reconstruction images at weeks 4, 8, and 12 show the perforation site of the bone defect (red arrow). Quantitative analysis of the area of interest (AOI) revealed that more new bone trabeculae were present in the S2 group, and the degree of bone trabecular dispersion was lower in the S2 group than in the other groups (Figure 7B).

2.3.2. Results of Histological Analysis. HE and Masson staining results of the samples at 4, 8, and 12 weeks after surgery are shown in Figure 8A,B. The S2 composite bone cement exhibited more new bone trabeculae than the other groups. Bone trabeculae were annular around the bone defect, and dense osteocytes, osteoblasts, and fibrous calluses were observed on the medial side. Significant angiogenesis was observed in the fibrous callus, which provided a good environment for bone regeneration at the defect site. A large number of fat vesicles were present in the bone defects of the control group, whereas they were fewer in the composite bone cement group, indicating that the cement material inhibited lipid differentiation and induced vascularization and osteogenic differentiation, thus generating more new bone trabeculae. These observations are consistent with the micro-CT results. At the later stage of bone repair (12 weeks), new bone trabeculae surrounding the bone defect were observed to transform into mature bone trabeculae, providing mechanical support in the defect area.

2.3.3. In Vivo Biosafety of the Composite Cement. The rats were euthanized 12 weeks after the operation and sliced. Hematoxylin and eosin (H&E) staining of the heart, liver, spleen, lung, and kidney tissues in each surgery group revealed the absence of abnormal or pathological changes compared to the sham group (Figure 9A). Tail venous blood was extracted from the rats at various time points for analyzing the liver and kidney functions and blood ion content to assess the in vivo biosafety of the materials (Figure 9B). Liver and kidney functions and calcium and phosphorus levels in the blood did not increase significantly as compared to those in the sham group. The results indicate that the composite cement did not cause ion accumulation in vivo and exhibited good biosecurity in vivo.

https://doi.org/10.1021/acsomega.3c00331
ACS Omega 2023, 8, 16809−16823

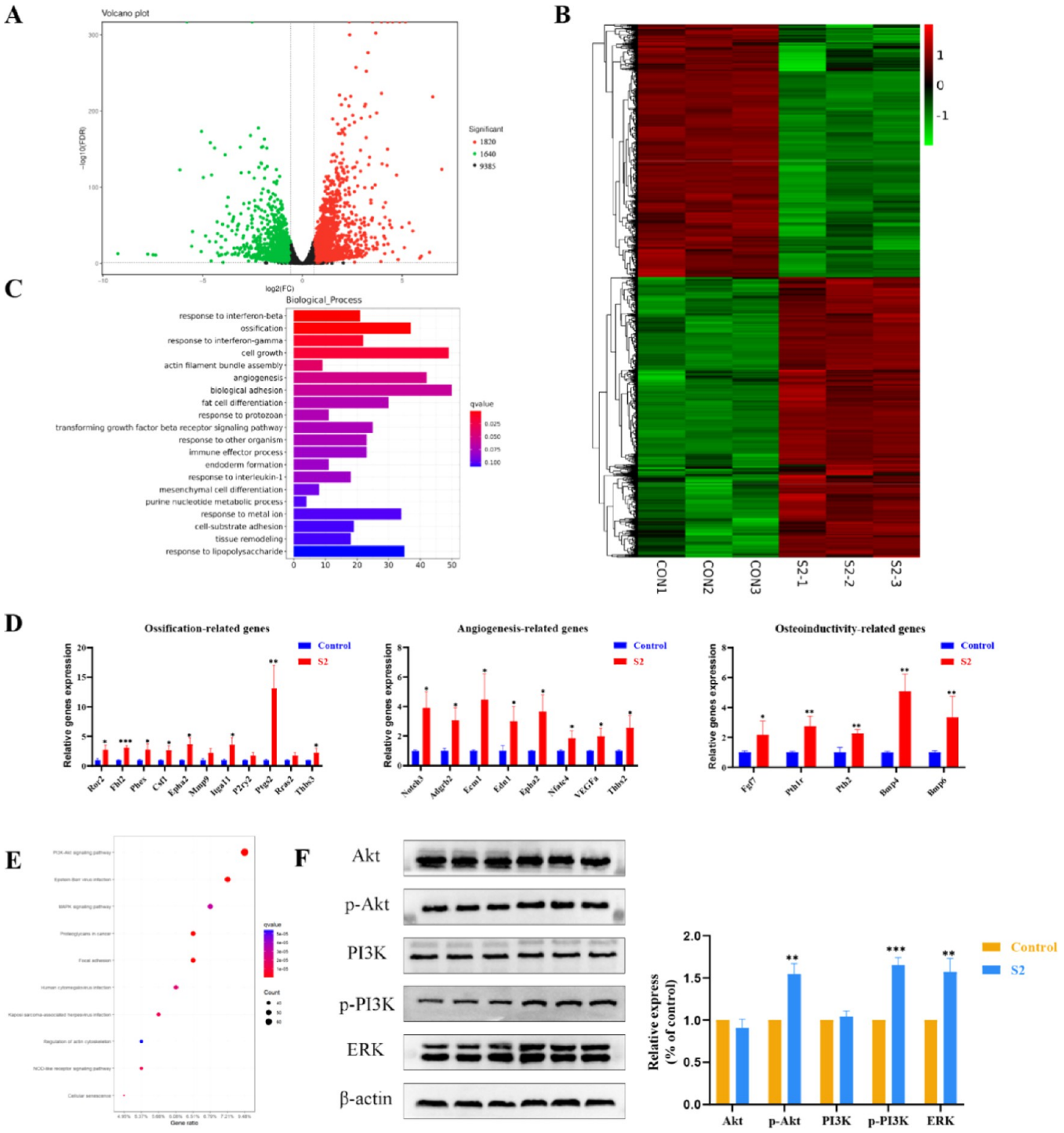

Figure 6. MSCs treated with osteogenic medium containing S2 bone cement extract (diluted twice) for 7 days, and the overall changes in gene expression were analyzed by RNA-seq. (A) Volcanic maps and (B) heat maps showed differences in gene expression in MSCs treated with S2 bone cement extract compared with untreated controls. (C) Gene ontology (GO) was presented through the biological process. (D) Quantitative validation of gene expression related to ossification, angiogenesis, and bone osteoinductivity. (E) Changes in the top 10 signaling pathways of MSCs in group S2, according to the KEGG enrichment analysis results. (F) Western blotting analysis results of key proteins in the PI3K/Akt and MAPK/Erk signaling pathways. (*$P < 0.05$, **$P < 0.01$, and ***$P < 0.001$, vs the control group, $n = 3$).

3. DISCUSSION

In the past few decades, bioceramics have been widely investigated as potential materials for repairing bone defects owing to their good biocompatibility, bone conductivity, and potential for promoting bone regeneration. This study comprehensively evaluated the feasibility of using a ternary CC/CHP/CSH composite bone cement as a new bone-repair material. The preparation and application of the composite bone cement and its potential for promoting bone regeneration are shown in Figure 10.

At present, calcium phosphate bone cement (CPC) is mainly used to reconstruct bone defects in craniomaxillofacial surgery because of its facile operation and satisfactory clinical perform-

https://doi.org/10.1021/acsomega.3c00331
ACS Omega 2023, 8, 16809−16823

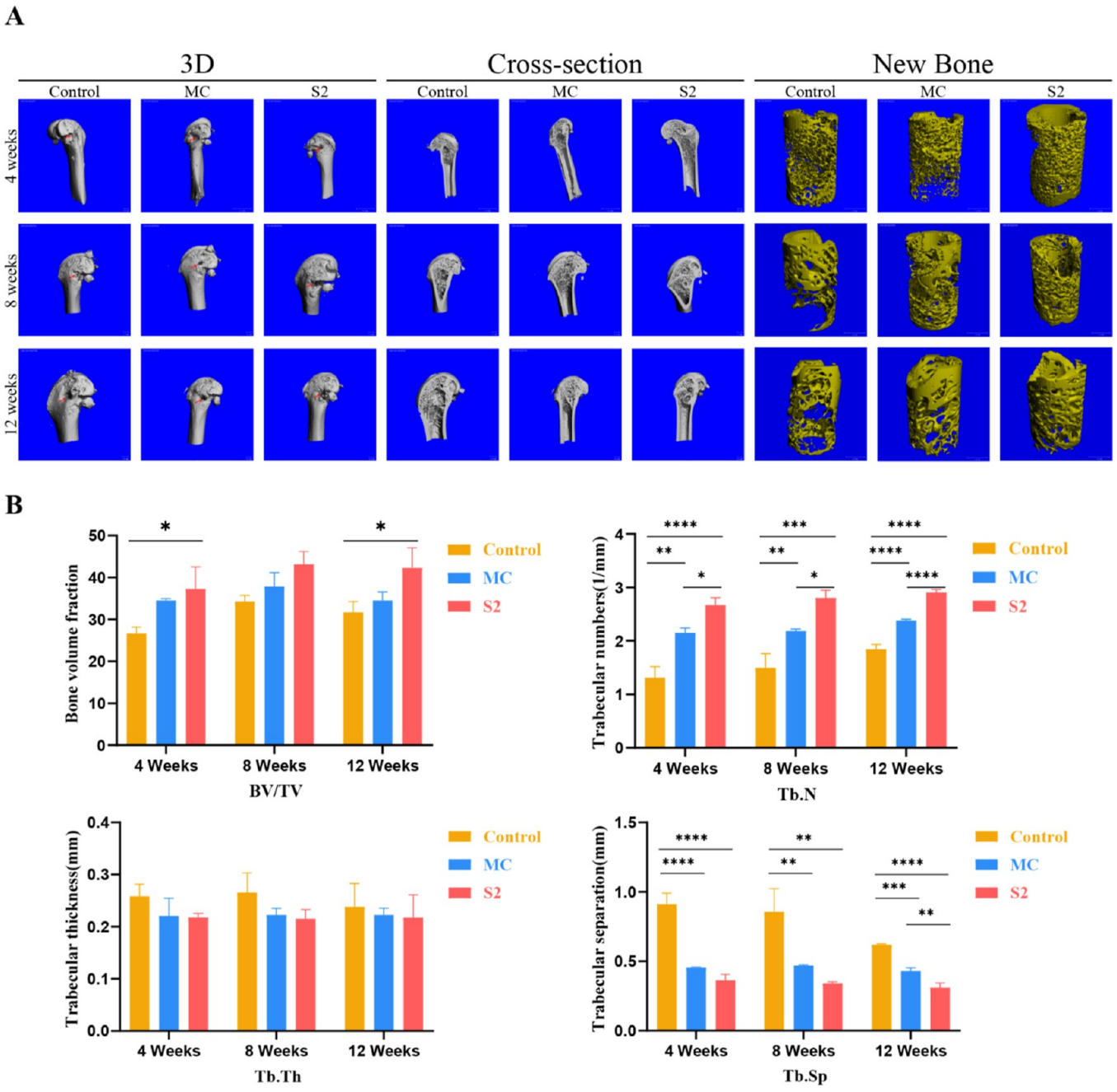

Figure 7. In vivo bone repair effect of the S2 bone cement group. (A) Micro-CT results of the in vivo bone defect repair process. (B) Analyses of in vivo bone defect repair effects by BV/TV, Tb.N, Tb.Th, and Tb.Sp at 4, 8, and 12 weeks. (*P < 0.05, **P < 0.01, ***P < 0.001, and ****P < 0.0001, vs control group, n = 3).

ance.[27−29] However, the filter extrusion phenomenon occurs when the CPC is delivered with only calcium phosphate particles and water as the liquid phase through a large-diameter needle or casing, which adversely affects the performance of the material after injection.[30−32] Citrate can be used as a dispersant, and its liquefaction effect can effectively improve the injectivity of the phosphate cement and the specific surface area of the CaP phase.[33−35] A large amount of citrate is present in human plasma, especially in bone tissue (57 mM), and the concentration of citrate present in the material (approximately 1.5 mM) is not harmful to bone regeneration. Adding calcium citrate to promote composite materials has no obvious toxic and side effects.[36] CSH is a typical bioabsorbable material. Owing to its advantages, such as high biocompatibility, bone conductivity, non-exothermic property, and X-ray detectability, it is considered as one of the most promising bone substitute materials. We further combined CSH with CC/CHP, which significantly improved the setting time and degradation rate of the cement. By changing the content of the semi-hydrated calcium sulfate, a composite bone cement with rapid setting characteristics (approximately 9−17 min) and a controlled degradation rate (53.6−74.9% at 12 weeks) was obtained. Compared to other single-component materials, our material is a ternary calcium-based bone cement, which is more abundant and exhibits better performance, such as a shorter setting time and better osteogenic ability.

https://doi.org/10.1021/acsomega.3c00331
ACS Omega 2023, 8, 16809−16823

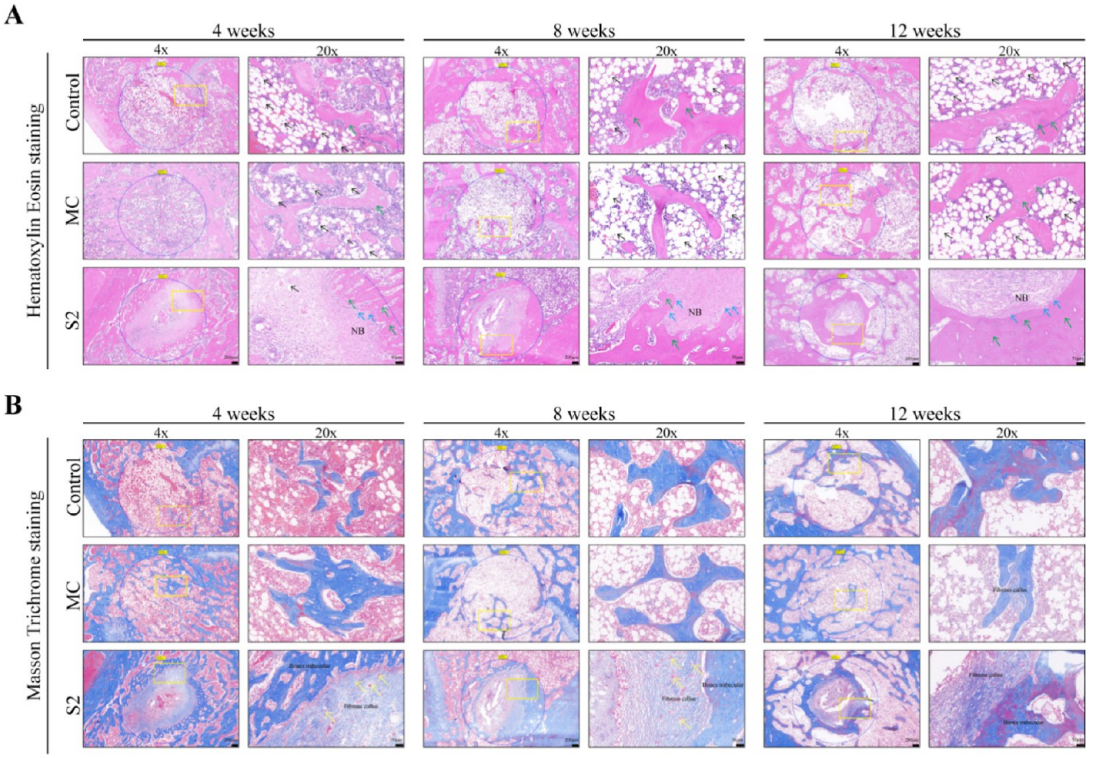

Figure 8. Histological analysis results of the control group, material control group, and S2 bone cement group. Low magnification (4×) and high magnification (20×) images of bone defect area are included. The images are arranged from left to right in each group of dyed samples. (A) Hematoxylin-Eosin staining, in which a large number of fat bubbles (black arrows) were observed in the bone defects of the control group and the material control group; parallelly, tight osteocytes (green arrows) and osteoblasts (blue arrows) were observed in the S2 bone cement group. (NB = new bone) (B) Masson Trichrome staining, in which dense bone trabeculae and fibrous calluses were formed at the bone defect area of the S2 bone cement group; meanwhile, and a large number of blood vessels were generated in the fibrous calluses (yellow arrow).

Ca^{2+} is an important homing signal in bone remodeling; it initiates and recruits a variety of cells to participate in bone remodeling.[37] A high Ca^{2+} concentration has been shown to stimulate the chemotaxis of osteoblasts toward the bone resorption site, where they mature into new bone-producing cells.[38] Therefore, early Ca^{2+} release is important for the repair of bone defects. In this study, the fastest degradation rate of the composite bone cement was observed in the first 2 weeks. Owing to the rapid degradation of the bone cement in the early stages, large amounts of Ca^{2+} and citric acid were released, which contributed to early bone regeneration. Studies have found that citric acid can mediate growth factors involved in angiogenesis and promote bone regeneration.[39,40] Many animal models have demonstrated that the incorporation of citric acid into biomaterials can promote bone formation; however, the role of extracellular citric acid in bone differentiation remains elusive.[22,41−43] In addition, citric acid acts as a Ca^{2+} chelator and is involved in many cellular processes with Ca^{2+} by regulating calmodulin, a major Ca^{2+} messenger.[44] However, the synergistic effect of citric acid and Ca^{2+} on bone repair requires further investigation.

OSX and Runx-2 are key regulators of osteogenic differentiation, and they regulate the expression of many osteogenic genes such as Col1a1 and OPN.[45−47] In our study, quantitative data on osteogenic gene expression by RT-PCR indicated significant increases in OSX, RUNX2, OPN, and Col1a1 in the experimental group as compared to those in the control group. Furthermore, RNA sequencing and western blot analysis revealed that the S2 composite cement activated the PI3K/Akt and MAPK/Erk signaling pathways, thereby upregulating the expression of downstream osteogenic genes to promote osteogenesis. The PI3K/Akt signaling pathway is involved in mitosis and in the regulation of various cellular physiological processes, including cell proliferation and apoptosis, and the maintenance and differentiation of stem cells.[48] The activation of the PI3K/Akt signaling pathway increases Runx-2 expression and promotes osteoblast proliferation, differentiation, and osteogenesis.[49] Further, MAPK/Erk signaling plays an important role in the activity of osteoblasts in vivo.[50] The activation of the MAPK/Erk signaling pathway promotes the expression of osteogenic genes (OSX and Col1a1), thus promoting new bone formation.[51,52] Previous studies have observed similarities between the actions of Ca^{2+} and citric acid, both of which promote osteogenesis by activating the MAPK/Erk signaling pathway.[53−55] This may cause the two to have a certain synergistic effect; however, further research is required to confirm this.

4. CONCLUSIONS

In this study, a CC/CHP/CSH composite bone cement with self-solidification and controlled degradation properties was successfully prepared for the first time and evaluated via physicochemical, in vitro, and in vivo biological tests. With the addition of CSH, the CC/CHP/CSH ternary calcium-based bone cement exhibited a faster setting time (10.45 min), higher mechanical strength (20.5 MPa), and a more suitable degradation rate (it degraded by ∼50% at 4 weeks). In vitro experiments demonstrated that the bone cement activated the PI3K/Akt and MAPK/Erk signaling pathways, promoting the proliferation and osteogenic differentiation of MSCs. In vivo

https://doi.org/10.1021/acsomega.3c00331
ACS Omega 2023, 8, 16809−16823

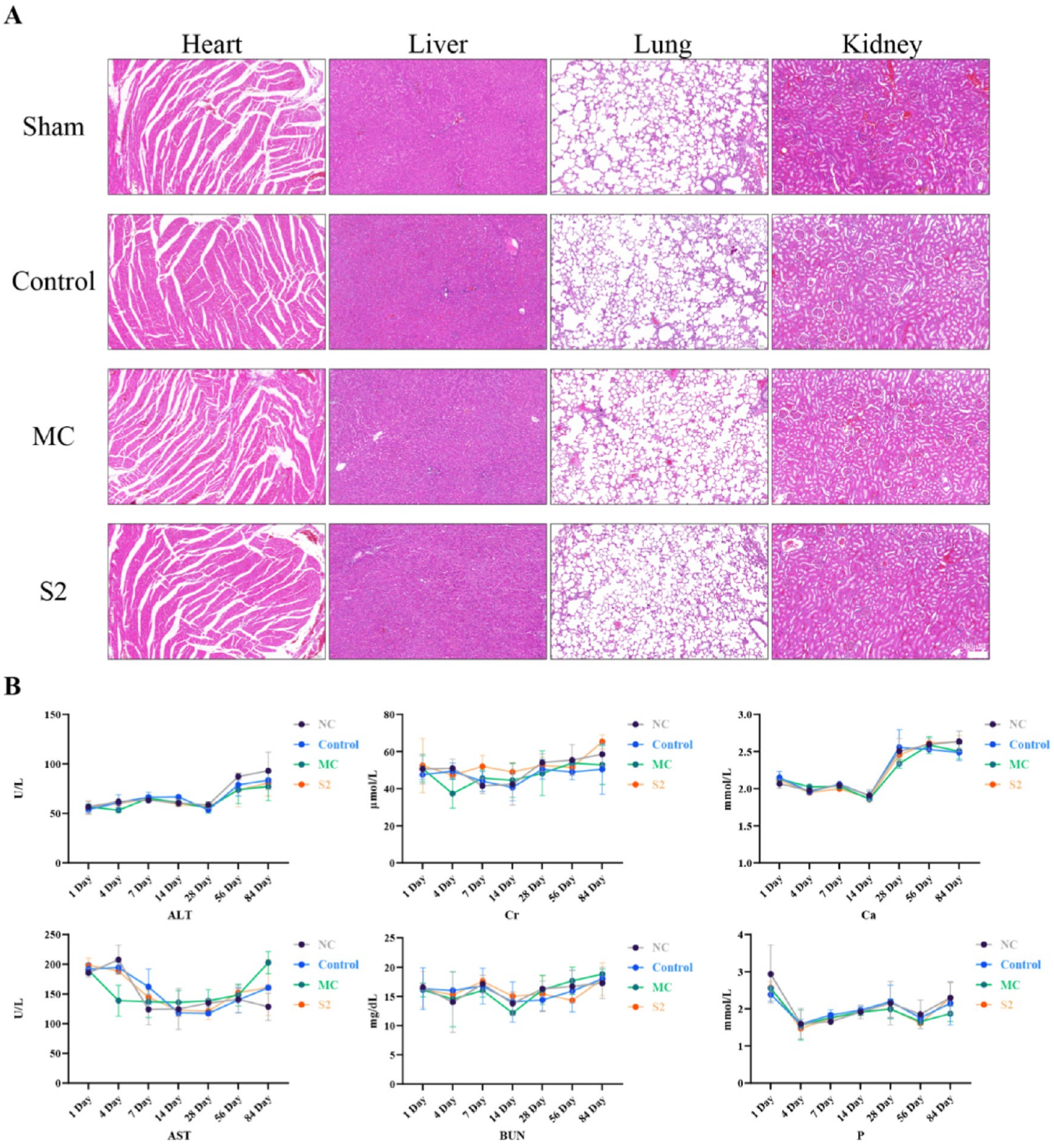

Figure 9. In vivo biological safety of the control group, material control group, and S2 bone cement group. (A) H&E staining of the heart, liver, lung, and kidney of rats in the sham operation group, control group, material control group, and S2 bone cement group 12 weeks after operation. (B) Liver and kidney functions and blood calcium and phosphorus concentrations of rats in each group at different times.

biosafety and osteogenic effect of the composite bone cement were confirmed using a rat model with femoral condylar bone defects. The CC/CHP/CSH ternary calcium-based bone cement was also observed to exhibit good biocompatibility and bone conductivity; therefore, it can be a new alternative for the clinical treatment of bone defects.

5. METHODS

5.1. Materials. CC and CHP were purchased from Aladdin Biochemical Technology Co. Ltd. (Shanghai, China), and CSH ($CaSO_4 \cdot 0.5H_2O$) was obtained from Sigma-Aldrich (St. Louis, MO, USA). Cell live/dead viability/cytotoxicity kit were obtained from Invitrogen (Carlsbad, CA, USA). An ALP staining kit and Alizarin red staining kit were supplied by Beijing Solarbio Science and Technology Co., Ltd. (China). Cell count

https://doi.org/10.1021/acsomega.3c00331
ACS Omega 2023, 8, 16809−16823

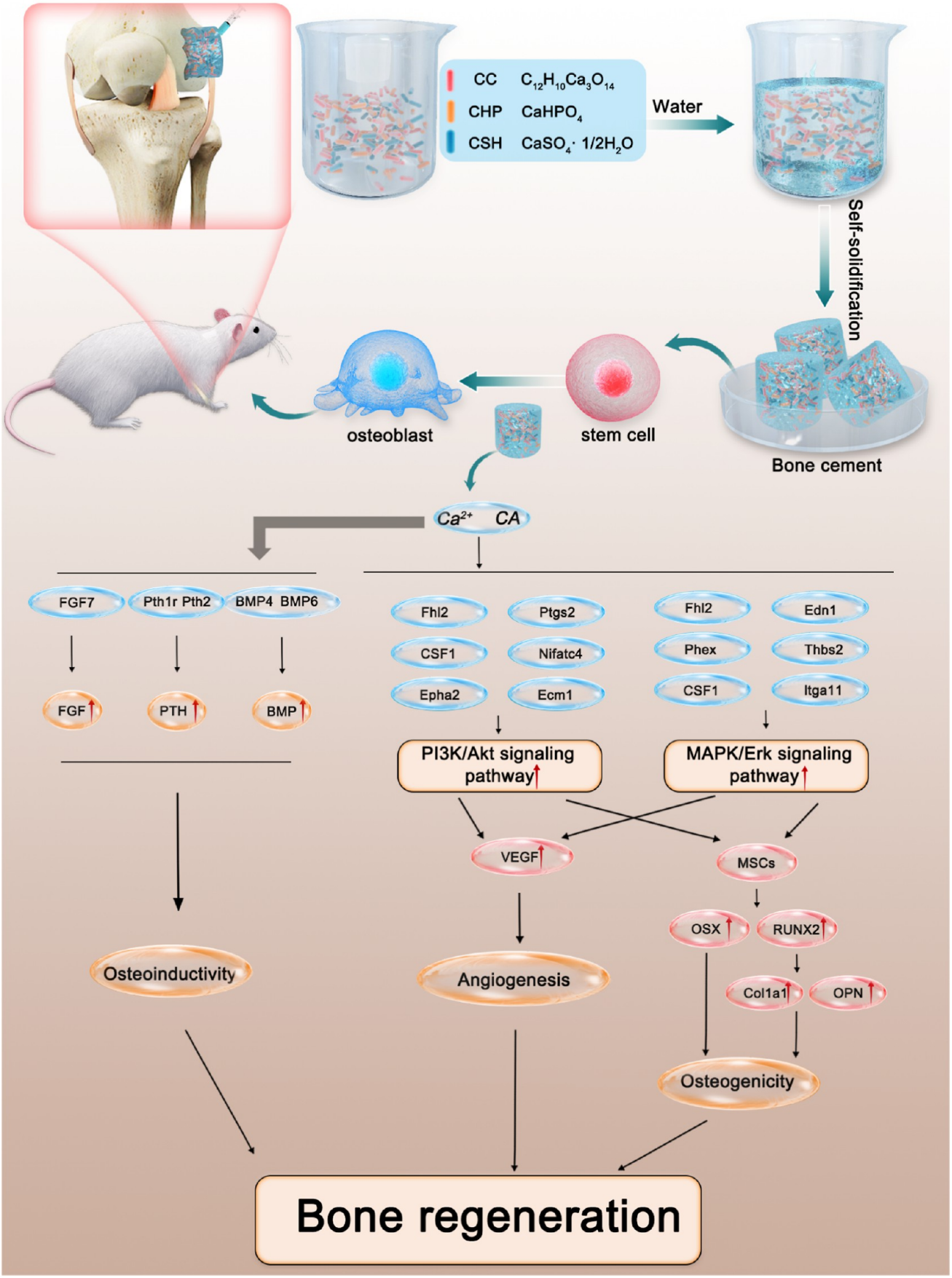

Figure 10. Preparation and application processes of bone cement, and its potential bone regeneration mechanism.

https://doi.org/10.1021/acsomega.3c00331
ACS Omega 2023, 8, 16809−16823

kit-8 was obtained from MCE (China), and mouse mesenchymal stem cell (MSC) line C3H10T1/2 was purchased from ATCC (Manassas, VA, USA). PI3K/Akt signaling pathway panel (ab283852, Abcam, USA), Anti-Erk1 antibody (ab32537, Abcam, USA), and β-Actin antibody (Cell Signaling Technology, USA) were used.

5.2. Preparation of the Ternary Cement. CC, CHP, and CSH were evenly mixed in a beaker according to the proportions listed in Table 2. Then, deionized water and whisks were added

Table 2. Proportions of the Bone Cements

	CC/g	CHG/g	CSH/g
S0	2.00	1.00	0.00
S1	2.00	1.00	1.00
S2	2.00	1.00	2.00
S3	2.00	1.00	3.00

with a liquid-to-solid ratio of ∼0.4 mL/g. Subsequently, the cements were loaded into cylindrical polytetrafluoroethylene molds, where they were turned into doughs. The samples were collected after 3 min.

5.3. Self-Setting Time and Compressive Strength. The setting time of each composite cement was measured using the Vicat apparatus according to the ISO 9597:2008 standard. The final setting time of the cement was defined as the time when a heavy needle left an indentation on the cement surface. The test was repeated at least three times for each cement type, and the average values of the results are reported. Cylindrical specimens (diameter: 6 mm; height: 7 mm) of the composite cement were used for testing. A mechanical tester was used to assess the compressive strength of the composite cement at 1, 6, 24, and 48 h after setting (REGER 30-50, Shenzhen Reger Co., Ltd., China).

5.4. Weight Loss and pH Measurement. The in vitro degradation of cement was evaluated based on the weight loss when immersed in a PBS. The cement (∼0.3 g) was incubated in a plastic bottle containing PBS at a liquid-to-solid ratio of approximately 1:30 and cultivated in a shaking water bath at 80 rpm and a constant temperature of 37 °C. The PBS was changed once a week. After the sample was soaked for different durations (1, 4, 7, 14, 28, 56, and 84 d), the pH of the solution in each bottle was measured using a pH meter (pH-25, Shanghai Laiqi, China). The soaked cement was then removed and dried at 60 °C for 12 h until a constant weight was obtained. To eliminate interference from water present in the cement, the original sample that was not soaked in PBS was dried under the same conditions and used as a control. Weight loss ratios were calculated using the following formula

$$\text{weight loss ratio}(\%) = (W_0 - W_t)/W_0 \times 100\%$$

where W_0 and W_t are the weights of the cement before and after immersion, respectively. The average porosity or weight loss of each sample was determined based on six measurements conducted under the same testing conditions. The average pH and weight loss rate of each sample were determined based on four measurements under the same test conditions.

5.5. Structural Characterization. The composition and morphology of the material were analyzed using the following methods: Fourier transform infrared (FT-IR) spectroscopy (iS10 FT-IR spectrometer, Negoli, USA) in the wave-number range of 400−4000 cm^{-1} at a resolution of 4 cm^{-1} and a signal-to-noise ratio of 50,000:1 (32 scans were made for recording each spectrum); X-ray photoelectron spectroscopy (Thermo Fisher 250Xi, USA); and XRD (D8 ADVANCE X-ray diffractometer from Brooke, Germany) performed in the 2θ range of 10−90° using Cu (wavelength: 1.5406 Å) and Co (wavelength: 1.79026 A) targets with a tube current of 40 mA and tube voltage of 40 kV.

5.6. In Vitro Bioactivity. After each group of cement was immersed in SBF for 7 days (37 °C, 80 rpm), the material surface was characterized. Cylindrical slabs of sterile cement (diameter: 6 mm; height: 7 mm) were prepared and soaked in SBF after drying for 1 day. The SBF was refreshed every 2 days. After 7 days of incubation, the cement slab was washed with deionized water, dried, and analyzed using SEM and EDS.

5.7. Cell Proliferation and Toxicity Tests. To evaluate the effect of materials on cells, a 6 mm × 7 mm composite cement sample was soaked in Dulbecco's modified Eagle's medium (DMEM) for 2 days. MSC cells of mice were inoculated in 6-well plates and then cultured in medium with cement immersion solution. Live/dead staining was performed on the 1st, 3rd, and 5th days, and the images of live/dead determination were observed using a fluorescence microscope (Nikon, Japan) under 488 nm laser excitation. Green fluorescence indicated living cells, and red fluorescence indicated dead cells.

Mice MSC cells were inoculated into 96-well plates with a cell density of 5000 cells/well. They were cultured according to the above treatment methods, and, simultaneously, CCK8 cell proliferation was detected (wavelength = 450 nm).

5.8. ALP and Alizarin Red Staining. The cement samples were immersed in osteogenic medium for 2 days. MSCs were inoculated in 24-well plates at a density of 70−80% and cultured in cement extracts containing different groups for 3, 5, 7, and 14 days. ALP staining was performed on days 3 and 5, and alizarin red staining on days 7 and 14.

5.9. Inductively Coupled Plasma Optical Emission Spectrometry and Ion Chromatography. The contents of Ca^{2+} and citric acid (CA) in the osteogenic culture medium containing the bone cement immersion solution were analyzed using inductively coupled plasma optical emission spectrometry (ICP-OES) and ion chromatography (IC) (Agilent ICP-OES730, USA) at a radio frequency power of 1.0 kW using argon as the carrier gas (plasma flow: 15 L/min, auxiliary gas flow: 1.5 L/min, nebulizer gas flow: 0.75 L/min, detector mode: axial, and calibration type: linear).

5.10. Real-Time PCR. Total RNA was isolated using the TRIzol reagent according to the manufacturer's instructions, complementary DNA was synthesized, and real-time PCR was performed. The primer sequence of RNA is shown in Table S1.

5.11. RNA Sequencing. The medium containing bone cement extract obtained by the above method was diluted twice and used to culture MC3H10T1/2 cells for 7 days. Blank osteogenic medium (no cement extract) was used as a control. The mRNA expression profiles were determined by the RNA sequencing analysis.

5.12. Western Blot. 20 μg of total protein was electrophoresed on a 10% SDS-PAGE gel according to the manufacturer's instructions. After the incubation of primary and secondary antibodies, WB bands were obtained via exposure. Finally, the protein bands were analyzed using ImageJ software.

5.13. Experimental Animals and Grouping. All animal experiments were approved by the Chongqing Medical University Animal Protection and Utilization Organization Committee (IACUC). Based on the in vitro results, the optimal

https://doi.org/10.1021/acsomega.3c00331
ACS Omega 2023, 8, 16809−16823

bone cement (S2) was selected for in vivo evaluation of osteogenic activity and biosafety. Furthermore, products having the same type of calcium sulfate were selected as controls for the clinical repair of large bone defects. Sixty 12 week old male rats were randomly divided into four groups: the sham operation group, control group (no materials), material control group (calcium sulfate cement), and experimental group (S2 cement). The operation was performed under sterile conditions. A cylindrical bone defect with a diameter of 3 mm and a depth of 5 mm was drilled into the lateral femoral condyle of the rat femur using a drill bit.

5.14. In Vivo Osteogenic Properties of the Cement. At 4, 8, and 12 weeks after surgery, the rats were euthanized to obtain the femur. Femoral condyles were analyzed using microcomputed tomography (microCT; Scanco micro-CT-100, Switzerland) and histological examination. The scan parameters are listed in Table S2. Three-dimensional (3D) images were reconstructed using ZKKS MicroCT 3.0 software, and the 1 mm diameter area of the most lateral bone defect was used as the area of interest (AOI). Bone volume fraction (BV/TV), trabecular number (Tb.N), trabecular separation (Tb.SP), and trabecular thickness (Tb.Th) were quantitatively analyzed using osteogenic indexes to evaluate the osteogenic activity of the material in vivo. After the scan was completed, the bone was decalcified, and the scanned femur was sectioned. H&E and Masson tri-color staining were used to evaluate the material for bone repair.

5.15. General Condition of Animals and In Vivo Biosafety. After 1, 4, 7, 14, 28, 56, and 84 days, blood was collected from the tail vein of rats in each group. The concentrations of Ca^{2+} and P in the blood samples and the liver and kidney functions of the rats were evaluated. Twelve weeks after the operation, the rat organs (heart, liver, spleen, lung, and kidney) were sampled, fixed with 4% paraformaldehyde, embedded, and stained with H&E staining to assess pathological changes to test the safety of materials in vivo (n = 5).

5.16. Statistical Analysis. GraphPad Prism 8.2 software was used for statistical analysis. The SPSS software package (version 22.0) was employed for statistical processing. The differences among multiple groups were analyzed by one-way analysis of variance, and the Tukey's test was used for comparisons between groups. Statistical significance was set at $P < 0.05$.

■ ASSOCIATED CONTENT

Supporting Information

The Supporting Information is available free of charge at https://pubs.acs.org/doi/10.1021/acsomega.3c00331.

SEM and EDS analyses of cements; in vivo testing of S2 cement in rat femoral defect; compressive strength of the S2 group in animals; RNA primer sequences; and details of the scanning procedure (PDF)

■ AUTHOR INFORMATION

Corresponding Authors

Yiting Lei − *The First Affiliated Hospital of Chongqing Medical University, Chongqing 400016, China*; Email: leiyit614@163.com

Yonggang Yan − *College of Physics, Sichuan University, Chengdu 610064, China*; Email: yan_yonggang@vip.163.com

Wei Huang − *The First Affiliated Hospital of Chongqing Medical University, Chongqing 400016, China*; orcid.org/0000-0002-8894-0982; Email: Huangweicqmuo@163.com

Authors

Shengwen Cheng − *The First Affiliated Hospital of Chongqing Medical University, Chongqing 400016, China*; orcid.org/0000-0001-5526-2444

Chen Zhao − *The First Affiliated Hospital of Chongqing Medical University, Chongqing 400016, China*

Senrui Liu − *The First Affiliated Hospital of Chongqing Medical University, Chongqing 400016, China*

Bowen Chen − *The First Affiliated Hospital of Chongqing Medical University, Chongqing 400016, China*

Hong Chen − *College of Physics, Sichuan University, Chengdu 610064, China*

Xuefeng Luo − *The First Affiliated Hospital of Chongqing Medical University, Chongqing 400016, China*

Li Wei − *The First Affiliated Hospital of Chongqing Medical University, Chongqing 400016, China*

Chengcheng Du − *The First Affiliated Hospital of Chongqing Medical University, Chongqing 400016, China*

Pengcheng Xiao − *The First Affiliated Hospital of Chongqing Medical University, Chongqing 400016, China*

Complete contact information is available at: https://pubs.acs.org/10.1021/acsomega.3c00331

Author Contributions

§S.C. and C.Z. contributed equally to this work.

Author Contributions

S.C. and C.Z. conducted the experiment and composed the manuscript. S.L., B.C., and H.C. helped in preparing the figures. X.L., L.W., C.D., and P.X. participated in the animal experiments. Y.L., Y.Y., and W.H. refined and arranged the contents of the manuscript. All authors approved the final manuscript.

Funding

This research was supported by the major project of Chongqing Municipal Education Commission (KJZD-M202100401).

Notes

The authors declare no competing financial interest.

All animal experiments were approved by the Animal Care and Use Organization Committee IACUC of Chongqing Medical University.

All authors are in agreement with the content of the manuscript and approved the final version of the manuscript.

The datasets used and analyzed during the current study are available from the corresponding author on reasonable request.

■ REFERENCES

(1) Doadrio, J. C.; Arcos, D.; Cabañas, M. V.; Vallet-Regí, M. Calcium Sulphate-Based Cements Containing Cephalexin. *Biomaterials* **2004**, *25*, 2629−2635.

(2) Nabiyouni, M.; Brückner, T.; Zhou, H.; Gbureck, U.; Bhaduri, S. B. Magnesium-Based Bioceramics in Orthopedic Applications. *Acta Biomater.* **2018**, *66*, 23−43.

(3) Zhao, Z.-H.; Ma, X.-L.; Zhao, B.; Tian, P.; Ma, J.-X.; Kang, J.-Y.; Zhang, Y.; Guo, Y.; Sun, L. Naringin-Inlaid Silk Fibroin/Hydroxyapatite Scaffold Enhances Human Umbilical Cord-Derived Mesenchymal Stem Cell-Based Bone Regeneration. *Cell Prolif.* **2021**, *54*, No. e13043.

(4) Gao, C.; Peng, S.; Feng, P.; Shuai, C. Bone Biomaterials and Interactions with Stem Cells. *Bone Res.* **2017**, *5*, 17059.

(5) Leach, J. K.; Whitehead, J. Materials-Directed Differentiation of Mesenchymal Stem Cells for Tissue Engineering and Regeneration. *ACS Biomater. Sci. Eng.* **2018**, *4*, 1115−1127.
(6) Maturavongsadit, P.; Wu, W.; Fan, J.; Roninson, I. B.; Cui, T.; Wang, Q. Graphene-incorporated hyaluronic acid-based hydrogel as a controlled Senexin A delivery system. *Biomater. Transl.* **2022**, *3*, 152−161.
(7) Laomeephol, C.; Ferreira, H.; Kanokpanont, S.; Luckanagul, J. A.; Neves, N. M.; Damrongsakkul, S. Osteogenic Differentiation of Encapsulated Cells in Dexamethasone-Loaded Phospholipid-Induced Silk Fibroin Hydrogels. *Biomater. Transl.* **2022**, *3*, 213−220.
(8) Zhao, X.; Ma, H.; Han, H.; Zhang, L.; Tian, J.; Lei, B.; Zhang, Y. Precision Medicine Strategies for Spinal Degenerative Diseases: Injectable Biomaterials with in Situ Repair and Regeneration. *Mater. Today Bio* **2022**, *16*, 100336.
(9) Li, Z.; Wang, Y.; Xu, Y.; Xu, W.; Zhu, X.; Chen, C. Efficacy Analysis of Percutaneous Pedicle Screw Fixation Combined with Percutaneous Vertebroplasty in the Treatment of Osteoporotic Vertebral Compression Fractures with Kyphosis. *J. Orthop. Surg. Res.* **2020**, *15*, 53.
(10) Sony, S.; Suresh Babu, S.; Nishad, K. V.; Varma, H.; Komath, M. Development of an Injectable Bioactive Bone Filler Cement with Hydrogen Orthophosphate Incorporated Calcium Sulfate. *J. Mater. Sci. Mater. Med.* **2015**, *26*, 31.
(11) Tansriratanawong, K.; Wongwan, P.; Ishikawa, H.; Nakahara, T.; Wongravee, K. Cellular Responses of Periodontal Ligament Stem Cells to a Novel Synthesized Form of Calcium Hydrogen Phosphate with a Hydroxyapatite-like Surface for Periodontal Tissue Engineering. *J. Oral Sci.* **2018**, *60*, 428−437.
(12) Farokhi, M.; Mottaghitalab, F.; Samani, S.; Shokrgozar, M. A.; Kundu, S. C.; Reis, R. L.; Fatahi, Y.; Kaplan, D. L. Silk Fibroin/Hydroxyapatite Composites for Bone Tissue Engineering. *Biotechnol. Adv.* **2018**, *36*, 68−91.
(13) Swetha, M.; Sahithi, K.; Moorthi, A.; Srinivasan, N.; Ramasamy, K.; Selvamurugan, N. Biocomposites Containing Natural Polymers and Hydroxyapatite for Bone Tissue Engineering. *Int. J. Biol. Macromol.* **2010**, *47*, 1−4.
(14) Manjula-Basavanna, A.; Duraj-Thatte, A. M.; Joshi, N. S. Robust Self-Regeneratable Stiff Living Materials Fabricated from Microbial Cells. *Adv. Funct. Mater.* **2021**, *31*, 2010784.
(15) Martins, M. A.; Santos, C.; Almeida, M. M.; Costa, M. E. V. Hydroxyapatite Micro- and Nanoparticles: Nucleation and Growth Mechanisms in the Presence of Citrate Species. *J. Colloid Interface Sci.* **2008**, *318*, 210−216.
(16) Martins, M. A.; Santos, C.; Almeida, M. M.; Costa, M. E. V. Hydroxyapatite Micro- and Nanoparticles: Nucleation and Growth Mechanisms in the Presence of Citrate Species. *J. Colloid Interface Sci.* **2008**, *318*, 210−216.
(17) Sun, D.; Chen, Y.; Tran, R. T.; Xu, S.; Xie, D.; Jia, C.; Wang, Y.; Guo, Y.; Zhang, Z.; Guo, J.; Yang, J.; Jin, D.; Bai, X. Citric Acid-Based Hydroxyapatite Composite Scaffolds Enhance Calvarial Regeneration. *Sci. Rep.* **2014**, *4*, 6912.
(18) Ghosh, P.; Rameshbabu, A. P.; Dhara, S. Citrate Cross-Linked Gels with Strain Reversibility and Viscoelastic Behavior Accelerate Healing of Osteochondral Defects in a Rabbit Model. *Langmuir* **2014**, *30*, 8442−8451.
(19) Sarda, S.; Fernández, E.; Nilsson, M.; Balcells, M.; Planell, J. A. Kinetic Study of Citric Acid Influence on Calcium Phosphate Bone Cements as Water-Reducing Agent: Citric Acid Influence on CPBCS. *J. Biomed. Mater. Res.* **2002**, *61*, 653−659.
(20) Tang, J.; Guo, J.; Li, Z.; Yang, C.; Xie, D.; Chen, J.; Li, S.; Li, S.; Kim, G. B.; Bai, X.; Zhang, Z.; Yang, J. A Fast Degradable Citrate-Based Bone Scaffold Promotes Spinal Fusion. *J. Mater. Chem. B* **2015**, *3*, 5569−5576.
(21) Han, T.; Carranza, F. A., Jr.; Kenney, E. B. Calcium Phosphate Ceramics in Dentistry: A Review of the Literature. *J. West Soc. Periodontol. Periodontal. Abstr.* **1984**, *32*, 88−108.
(22) Zaner, D. J.; Yukna, R. A. Particle Size of Periodontal Bone Grafting Materials. *J. Periodontol.* **1984**, *55*, 406−409.
(23) Chen, Z.; Liu, H.; Liu, X.; Lian, X.; Guo, Z.; Jiang, H.-J.; Cui, F.-Z. Improved Workability of Injectable Calcium Sulfate Bone Cement by Regulation of Self-Setting Properties. *Mater. Sci. Eng., C* **2013**, *33*, 1048−1053.
(24) Lazáry, A.; Balla, B.; Kósa, J. P.; Bácsi, K.; Nagy, Z.; Takács, I.; Varga, P. P.; Speer, G.; Lakatos, P. Effect of Gypsum on Proliferation and Differentiation of MC3T3-E1 Mouse Osteoblastic Cells. *Biomaterials* **2007**, *28*, 393−399.
(25) Tay, B. K.; Patel, V. V.; Bradford, D. S. Calcium Sulfate- and Calcium Phosphate-Based Bone Substitutes. Mimicry of the Mineral Phase of Bone. *Orthop. Clin. N. Am.* **1999**, *30*, 615−623.
(26) Thomas, M. V.; Puleo, D. A. Calcium Sulfate: Properties and Clinical Applications. *J. Biomed. Mater. Res., Part B* **2009**, *88B*, 597−610.
(27) Kamerer, D. B.; Hirsch, B. E.; Snyderman, C. H.; Costantino, P.; Friedman, C. D. Hydroxyapatite Cement: A New Method for Achieving Watertight Closure in Transtemporal Surgery. *Am. J. Otol.* **1994**, *15*, 47−49.
(28) Kveton, J. F.; Friedman, C. D.; Piepmeier, J. M.; Costantino, P. D. Reconstruction of Suboccipital Craniectomy Defects with Hydroxyapatite Cement: A Preliminary Report. *Laryngoscope* **1995**, *105*, 156−159.
(29) Kveton, J. F.; Friedman, C. D.; Costantino, P. D. Indications for Hydroxyapatite Cement Reconstruction in Lateral Skull Base Surgery. *Am. J. Otol.* **1995**, *16*, 465−469.
(30) Bohner, M. Theoretical considerations on the injectability of calcium phosphate cements *Proceedings on the 17th European Conference on Biomaterials*: Barecelona, Spain, 2002; p 124.
(31) Khairoun, I.; Boltong, M. G.; Driessens, F. C.; Planell, J. A. Some Factors Controlling the Injectability of Calcium Phosphate Bone Cements. *J. Mater. Sci. Mater. Med.* **1998**, *9*, 425−428.
(32) Leroux, L.; Hatim, Z.; Frèche, M.; Lacout, J. L. Effects of Various Adjuvants (Lactic Acid, Glycerol, and Chitosan) on the Injectability of a Calcium Phosphate Cement. *Bone* **1999**, *25*, 31S−34S.
(33) Sarda, S.; Fernandez, E.; Nilson, M.; Balcells, M.; Planell, J. A. Kinetic effect of citric acid influence on calcium phosphate bone cements as water reducing agent. *J. Biomed. Mater. Res.* **2002**, *61*, 653−659.
(34) Dai, H. L.; Yan, Y. H.; Feng, L. Y.; Li, S. P.; He, J. H. Basic properties of calcium phosphate cement containing different concentrations of citric acid solution. *Trans. Nonferrous Met. Soc. China* **2002**, *12*, 475−479.
(35) Gbureck, U.; Barralet, J. E.; Spatz, K.; Grover, L. M.; Thull, R. Ionic Modification of Calcium Phosphate Cement Viscosity. Part I: Hypodermic Injection and Strength Improvement of Apatite Cement. *Biomaterials* **2004**, *25*, 2187−2195.
(36) Leeuwenburgh, S. C. G.; Ana, I. D.; Jansen, J. A. Sodium Citrate as an Effective Dispersant for the Synthesis of Inorganic-Organic Composites with a Nanodispersed Mineral Phase. *Acta Biomater.* **2010**, *6*, 836−844.
(37) Dvorak, M. M.; Riccardi, D. Ca2+ as an Extracellular Signal in Bone. *Cell Calcium* **2004**, *35*, 249−255.
(38) Chai, Y. C.; Carlier, A.; Bolander, J.; Roberts, S. J.; Geris, L.; Schrooten, J.; Van Oosterwyck, H.; Luyten, F. P. Current Views on Calcium Phosphate Osteogenicity and the Translation into Effective Bone Regeneration Strategies. *Acta Biomater.* **2012**, *8*, 3876−3887.
(39) Mycielska, M. E.; Milenkovic, V. M.; Wetzel, C. H.; Rümmele, P.; Geissler, E. K. Extracellular Citrate in Health and Disease. *Curr. Mol. Med.* **2015**, *15*, 884−891.
(40) Iacobazzi, V.; Infantino, V. Citrate–New Functions for an Old Metabolite. *Biol. Chem.* **2014**, *395*, 387−399.
(41) Tran, R. T.; Wang, L.; Zhang, C.; Huang, M.; Tang, W.; Zhang, C.; Zhang, Z.; Jin, D.; Banik, B.; Brown, J. L.; Xie, Z.; Bai, X.; Yang, J. Synthesis and characterization of biomimetic citrate-based biodegradable composites. *J. Biomed. Mater. Res., Part A* **2014**, *102*, 2521−2532.
(42) Schneiders, W.; Reinstorf, A.; Pompe, W.; Grass, R.; Biewener, A.; Holch, M.; Zwipp, H.; Rammelt, S. Effect of Modification of Hydroxyapatite/Collagen Composites with Sodium Citrate, Phospho-

https://doi.org/10.1021/acsomega.3c00331
ACS Omega 2023, 8, 16809−16823

serine, Phosphoserine/RGD-Peptide and Calcium Carbonate on Bone Remodelling. *Bone* **2007**, *40*, 1048−1059.
(43) Guo, Y.; Tran, R. T.; Xie, D.; Wang, Y.; Nguyen, D. Y.; Gerhard, E.; Guo, J.; Tang, J.; Zhang, Z.; Bai, X.; Yang, J. Citrate-Based Biphasic Scaffolds for the Repair of Large Segmental Bone Defects: Citrate-Based Biphasic Scaffolds. *J. Biomed. Mater. Res., Part A* **2015**, *103*, 772−781.
(44) Neufeld, T.; Eisenstein, M.; Muszkat, K. A.; Fleminger, G. A Citrate-Binding Site in Calmodulin. *J. Mol. Recognit.* **1998**, *11*, 20−24.
(45) Ducy, P.; Zhang, R.; Geoffroy, V.; Ridall, A. L.; Karsenty, G. Osf2/Cbfa1: A Transcriptional Activator of Osteoblast Differentiation. *Cell* **1997**, *89*, 747−754.
(46) Yin, N.; Zhu, L.; Ding, L.; Yuan, J.; Du, L.; Pan, M.; Xue, F.; Xiao, H. MiR-135-5p Promotes Osteoblast Differentiation by Targeting HIF1AN in MC3T3-E1 Cells. *Cell. Mol. Biol. Lett.* **2019**, *24*, 51.
(47) Nakashima, K.; Zhou, X.; Kunkel, G.; Zhang, Z.; Deng, J. M.; Behringer, R. R.; de Crombrugghe, B. The Novel Zinc Finger-Containing Transcription Factor Osterix Is Required for Osteoblast Differentiation and Bone Formation. *Cell* **2002**, *108*, 17−29.
(48) Martini, M.; De Santis, M. C.; Braccini, L.; Gulluni, F.; Hirsch, E. PI3K/AKT Signaling Pathway and Cancer: An Updated Review. *Ann. Med.* **2014**, *46*, 372−383.
(49) Majidinia, M.; Sadeghpour, A.; Yousefi, B. The Roles of Signaling Pathways in Bone Repair and Regeneration. *J. Cell. Physiol.* **2018**, *233*, 2937−2948.
(50) Camal Ruggieri, I. N.; Cícero, A. M.; Issa, J. P. M.; Feldman, S. Bone Fracture Healing: Perspectives According to Molecular Basis. *J. Bone Miner. Metabol.* **2021**, *39*, 311−331.
(51) Cui, D.; Xiao, J.; Zhou, Y.; Zhou, X.; Liu, Y.; Peng, Y.; Yu, Y.; Li, H.; Zhou, X.; Yuan, Q.; Wan, M.; Zheng, L. Epiregulin Enhances Odontoblastic Differentiation of Dental Pulp Stem Cells via Activating MAPK Signalling Pathway. *Cell Prolif.* **2019**, *52*, No. e12680.
(52) Barbuto, R.; Mitchell, J. Regulation of the Osterix (Osx, Sp7) Promoter by Osterix and Its Inhibition by Parathyroid Hormone. *J. Mol. Endocrinol.* **2013**, *51*, 99−108.
(53) Shao, D.; Lu, M.; Xu, D.; Zheng, X.; Pan, Y.; Song, Y.; Xu, J.; Li, M.; Zhang, M.; Li, J.; Chi, G.; Chen, L.; Yang, B. Carbon Dots for Tracking and Promoting the Osteogenic Differentiation of Mesenchymal Stem Cells. *Biomater. Sci.* **2017**, *5*, 1820−1827.
(54) Huang, Z.; Cheng, S.-L.; Slatopolsky, E. Sustained Activation of the Extracellular Signal-Regulated Kinase Pathway Is Required for Extracellular Calcium Stimulation of Human Osteoblast Proliferation. *J. Biol. Chem.* **2001**, *276*, 21351−21358.
(55) Lai, C. F.; Chaudhary, L.; Fausto, A.; Halstead, L. R.; Ory, D. S.; Avioli, L. V.; Cheng, S. L. Erk Is Essential for Growth, Differentiation, Integrin Expression, and Cell Function in Human Osteoblastic Cells. *J. Biol. Chem.* **2001**, *276*, 14443−14450.

https://doi.org/10.1021/acsomega.3c00331
ACS Omega 2023, 8, 16809−16823